

# Mode Localization Experiments on a Ribbed Antenna

M. B. Levine-West\* and M. A. Salama†

*Jet Propulsion Laboratory, California Institute of Technology, Pasadena, California 91125*

In this paper, the mode localization (ML) phenomenon is investigated experimentally and analytically to determine the influence of its parameters. For this purpose, a full-scale 12-rib loosely coupled antenna testbed with small imperfections is dynamically tested for various levels of inter-rib coupling stiffness and excitation force. The experimental results are described herein. Using a simplified numerical model of the structure, a sensitivity analysis of the modal behavior is also performed. The numerical and experimental results are shown to agree remarkably well, thereby providing conclusive validation of the ML phenomenon on a testbed having the dynamic characteristics of space structures.

## I. Introduction

**M**ODE localization (ML) is a dynamic phenomenon associated with weakly coupled periodic structures, and resulting from small imperfections ( $\leq 5\%$ ) which perturb the periodicity. Such imperfections typically result from random manufacturing or assembly imprecisions. Numerous numerical and analytical investigations have shown that such structures can be susceptible to displaying modal deformations which are quite different from those expected if the periodic structure had no imperfections. In extreme cases of ML, the modal energy and deformations are confined to a single component, instead of having the periodic distribution predicted for a perfect structure. If not adequately incorporated into the analysis model, ignoring ML could have adverse effects on the design of active control systems. It could compromise system identification schemes based on periodicity, or could lead to erroneous results if accurate shape control is required. Also, the confinement of the vibrational energy to particular components could yield dangerously high stress levels. Conversely, ML could be advantageous in reducing vibrations in specific regions of a structure.

However, the existence of ML or the influence of its parameters have not yet been demonstrated on an actual space-like structure. This provided the motivation for the research described herein, with the objective of demonstrating analytically and experimentally the degree to which actual structures—having the complexity and dynamic characteristics of space structures—are susceptible to mode localization.<sup>1</sup> For this purpose, the antenna testbed shown in Fig. 1 was used to investigate and ascertain the existence of ML.

After a brief overview of the theory of ML, the testbed facility, the data acquisition system, and the data-reduction software are described, as well as the identified and measured small structural imperfections. A preliminary analysis of the sensitivity of the modal properties to variations in the inter-rib stiffness was conducted. A description of the model with the actual imperfections and conclusions derived from the numerical modal analysis are presented. Based on these conclusions, certain modes were targeted for the experiments and were excited at several forcing levels for various amounts of inter-rib stiffness. The impact of nonlinear dynamic response and

structural damping on the degree of ML are considered in the analysis of the experimental results. The numerical and experimental results are then compared, and their correlation is discussed. A video of the experiments has also been produced which visually depicts the experimental setup and procedure, and which clearly demonstrates the existence of mode localization in the antenna as a function of the inter-rib coupling stiffness.<sup>13</sup>

## II. Mode Localization

Many analytical investigations have established the effects of small imperfections on the modal response of loosely coupled periodic structures.<sup>1-8</sup> The theory of mode localization will not be rederived, only the major conclusions relevant to the experiments are described hereafter. The modes of a structure assembled in a periodic or cyclic array of identical components are known to cluster in many groups or bands. The band number refers to the modes of the components. For instance, in the structure of Fig. 1, band 1 corresponds to the modal cluster in which each rib deforms in the first cantilever bending mode, and band 2 refers to the modal cluster in which each rib deforms in the second cantilever bending mode. The number of modes within each band is equal to the number of components forming the structure. Inside each band, the distinct components deform with the same mode shape, and each mode of the band describes the phase difference between the individual components (i.e., circular wave number). In general, the first mode of the band represents all of the components deforming in phase (i.e., umbrella mode for the ribbed antenna), whereas in the last mode of the band all of the components are moving 180 deg out-of-phase. In the case of cyclically symmetric structures, the modes inside each band are degenerate if there are no imperfections.

Small structural or coupling imperfections annihilate the modal degeneracy, but spawn pairs of closely spaced modes

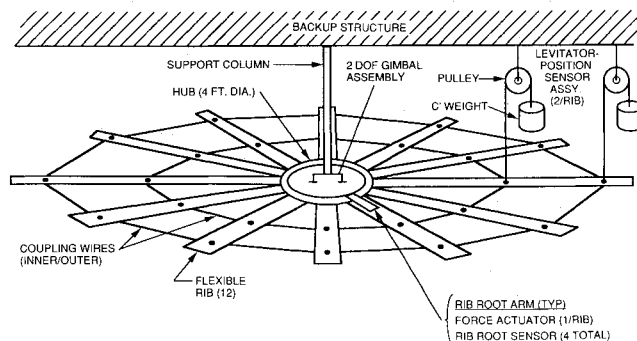


Fig. 1 JPL/AF 12-rib antenna testbed used for the ML experiments.<sup>9</sup>

Received Feb. 6, 1992; presented as Paper 92-2453 at the AIAA/ASME/ASCE/AHS/ASC 33rd Structures, Structural Dynamics, and Materials Conference, Dallas, TX, April 13-15, 1992; revision received Jan. 12, 1993; accepted for publication Jan. 12, 1993. Copyright © 1993 by the American Institute of Aeronautics and Astronautics, Inc. The U.S. Government has a royalty-free license to exercise all rights under the copyright claimed herein for Governmental purposes. All other rights are reserved by the copyright owner.

\*Member of Technical Staff, 4800 Oak Grove Drive, MS 157-316.

†Technical Group Leader, 4800 Oak Grove Drive, MS 157-316.

characterized by disorder in the expected modal deformations had the structure been perfect. In extreme cases, the modal deformation can be "localized" to a single element instead of being extended throughout the complete structure. Using the convention of Pierre et al.,<sup>3</sup> a mode is said to localize if the amplitude of its mode shape at any location on the structure is less than 10% of the expected ideal mode shape. Analytical and numerical investigations have shown that a periodic structure is prone to have localized modes if the coupling stiffness between the imperfect components is much less than the individual structural stiffness of the components themselves. In the limiting case where there is no coupling, the components vibrate independently of each other. The degree of localization decreases as the level of intercomponent coupling is increased, and localization disappears as the relative stiffness of the coupling becomes extremely high.<sup>3</sup>

Typically, the degree of imperfection resulting from assembly and manufacturing imperfections is considered to be approximately 5% or less for most ML parameters. It is assumed that larger imperfections could not qualify as perturbations to quasiperiodic structures, although modal irregularities may still be observed. In effect, the variations in the structural properties that engender ML are all those that affect the modal frequencies and response. For components modeled as beams, ML is most sensitive to imperfections in the beam thickness and length.<sup>1</sup> Just as variations of these individual parameters lead to modal perturbations, and ultimately to ML in the overall structure, suitable combinations of these perturbed parameters should also lead to delocalization of the loosely coupled imperfect structure.

The degree of modal density and coupling can be measured by the modal bandwidth. For modal band  $j$ , it is defined by Bendiksen as<sup>2</sup>

$$\Delta\lambda_j = \frac{\omega_{\max,j}^2 - \omega_{\min,j}^2}{\omega_{\min,j}^2} \quad (1)$$

where  $\omega_{\max,j}$  and  $\omega_{\min,j}$  are the upper and lower frequencies of band  $j$ . It can be shown that for single degree-of-freedom components,  $\Delta\lambda_j$  increases proportionally to the coupling stiffness.<sup>5</sup> The smaller  $\Delta\lambda_j$  becomes, the looser the coupling, and the more the modes contained within the band are sensitive to imperfections are likely to localize. It has been shown numerically that  $\Delta\lambda_j$  decreases with increasing modal group  $j$ , and that higher modal groups are more likely to localize. It is thus possible for a loosely coupled structure to have fully extended modes in its lower modal bands, but to have deformed or localized modes in its higher modal bands. The degree of ML also increases as a function of the total number  $N$  of ribs forming the structure, as has been confirmed analytically for ribbed antennas.<sup>2</sup> Furthermore, numerical analysis has shown that modes located at the edges of the bands are more sensitive to imperfections and are more likely to localize than those situated inside the band. Thus, the so-called umbrella mode and the 180 deg out-of-phase mode are those most susceptible to ML.<sup>5</sup>

The effects of the coupling location has been considered by Cha and Pierre.<sup>6</sup> They demonstrated that when the coupling constraint is located at the node of a particular modal group, then that band will be very susceptible to ML. Intuitively, if the coupling constraint is located at the modal nodes of the individual components, the vibrating structure will not "feel" the coupling in the corresponding modal band since there are no deformations at the coupling points. Hence, in effect the coupling for that particular band is very weak and can lead to strong localization. Conversely, it may be inferred that if the coupling constraint is located at the maximum deformation point of the component mode, then localization is restrained in the corresponding modal band of the structure. This question has not been investigated analytically in the literature, but could be useful in reducing ML in critical situations.

Lust et al.<sup>8</sup> have studied the effects of modal damping on the localized response. Although both damping and localiza-

tion decrease the modal response in certain regions of the structure, these two phenomenon should not be confused. Damping results in decreased modal amplitudes because of energy *absorption*, whereas localization results in decreased amplitudes because of energy *confinement*. It was shown numerically that modal damping of the order of 1% lessens the difference in the modal response between the ideal and the localized structures.

The primary purpose of the following experiments is to verify that ML is a true phenomenon which can be observed and measured experimentally in realistic structures that are dynamically similar to space structures. To this end, this section presented the qualitative impact of those parameters which could be used to provoke ML in the existing testbed. A more detailed description of the numerical methods, models, and quantitative results is provided in the references.

### III. Test Facility

#### Flexible Antenna Testbed

The test structure used for the ML experiment is a flexible 12-rib, 5.75-m-diam, circular antenna-like structure with a gimballed central hub (Fig. 1). This structure was originally designed for adaptive control, static shape control, and model identification experiments. The original configuration was slightly altered for the ML tests, and a very stiff brace was placed under the gimballed central hub to prevent rotations and to minimize inter-rib coupling through the hub. Only the structural information relevant to the ML tests is reported below. More detailed description of the antenna testbed is given by Vivian et al.<sup>9</sup>

The test structure consists of 12 flexible ribs which are clamped to a 1.22-m-diam central hub. These ribs are made of 0.223-cm-thick steel strap, and are 7.62-cm wide and 2.25-m long. Nine removable 0.033-kg stud masses are evenly spaced along each rib. Twenty-four levitator assemblies are used to suspend each rib at two locations to minimize the rms of the deflection due to gravity. The levitator assembly consists of a 15.24-cm-diam ball-bearing pulley and a counterweight which is cabled around the pulley and attached to the rib (Fig. 1). Each counterweight is individually matched to its specific rib and levitator position.

The ribs are coupled in the circumferential direction by two rings of constant-force coupling wires. These wires are assembled to springs at either ends, and are then connected to the ribs at the inner and outer levitator positions (Fig. 1). Changing the inter-rib coupling tension is equivalent to varying the wire stiffness. For the ML experiment, a special spring mechanism was designed to produce variable inter-rib tensions which can be accurately measured between 0.56 N (0.125 lbf) and 44.48 N (10 lbf). In their original configuration, the coupling springs in the inner ring are tensioned to 4.45 N (1 lbf), and those in the outer ring are tensioned to 2.22 N (0.5 lbf). This will later be referred to as the nominal coupling tension. Inter-rib tensions higher than three times the nominal value could possibly buckle the ribs, and thus were not attempted.<sup>9</sup>

Each rib can be excited by one of the 12 rib-root force voice-coil actuators (Fig. 1). The ribs can either be excited individually, all 12 at a time, or with any combination in between. Phase shifts between the ribs can also be introduced in the excitation forces. Forces up to  $\pm 2$  N (8.96 lbf) can be generated by these actuators. Twenty-four 12-bit optical encoders are nested into each of the pulley rotation shafts (Fig. 1), and record the displacement along each rib at the inner and outer coupling-ring locations. The measured displacements are accurate to within 0.266 mm (1/10 in.).

The data acquisition system (DAS) sends commands to the actuators and samples the motions detected by the sensors. The extensive supporting software enables, among other capabilities, to remove any existing displacement bias within the recording sensors, to define the force-excitation pattern and level at each ribroot, and to select the frequency range of sine-sweep tests or the desired frequency of tuned sine-dwell

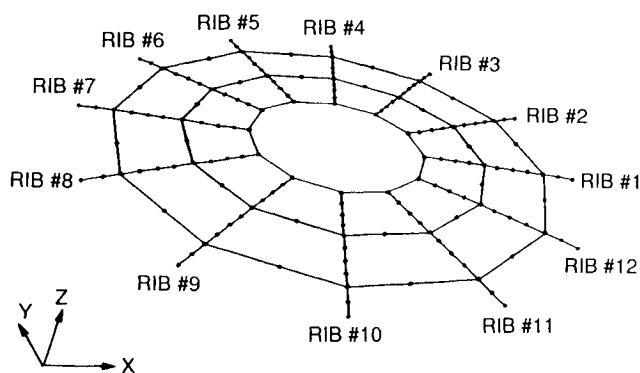


Fig. 2 Finite element model of the 12-rib space-reflector testbed.

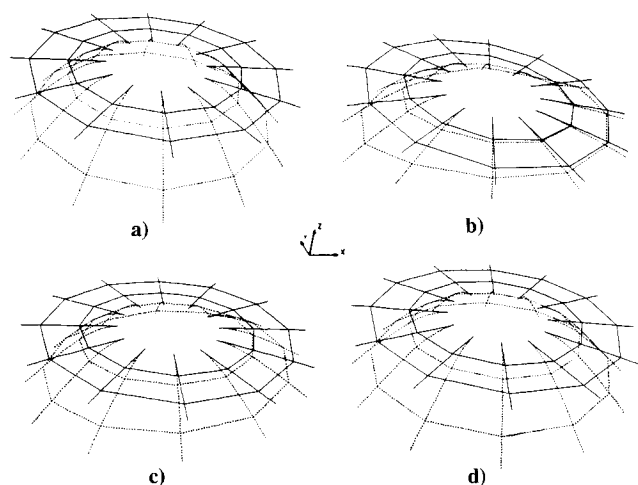


Fig. 3 Mode 1-band 1 deformations of the numerical 12-rib antenna model: a) the ideal structure at nominal coupling,  $f = 0.228$  Hz; b) the actual structure with measured imperfections at quarter coupling,  $f = 0.228$  Hz; c) nominal coupling,  $f = 0.216$  Hz; and d) triple coupling,  $f = 0.173$  Hz.

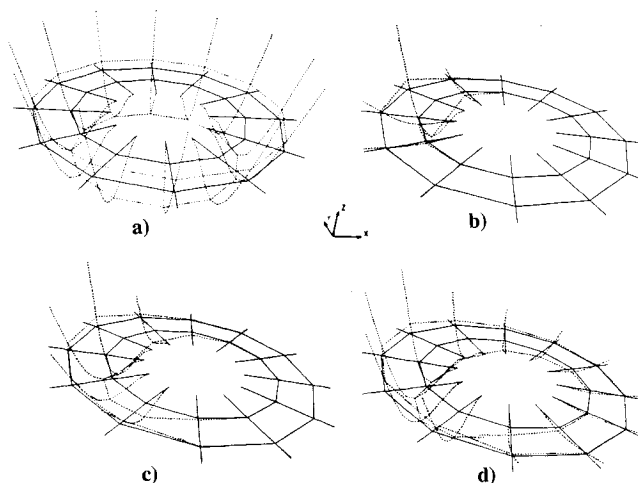


Fig. 4 Mode 1-band 2 deformations of the numerical 12-rib antenna model: a) the ideal structure at nominal coupling,  $f = 0.1516$  Hz; b) the actual structure with measured imperfections at quarter coupling,  $f = 1.480$  Hz; c) nominal coupling,  $f = 0.1473$  Hz; and d) triple coupling,  $f = 1.442$  Hz.

tests. The DAS is presently set up to record and store 1001 points of time-history data from each of the 44 actuators and sensors.

#### Data Processing and Modal Parameter Identification

The data recorded from the 12 force actuators at the rib roots and the 24 optical encoders measuring the displacement time histories at two points along each rib are used to determine the modal properties of the structure. The software used, MODE-ID, was initially developed by Beck<sup>10</sup> for earthquake engineering purposes. MODE-ID is a time-domain, multiple-input multiple-output system-identification method that identifies the modal frequencies, damping, mode shapes, and participation factors of a linear MDOF dynamic system with classical normal modes. It can also identify the initial modal displacement and velocity if the structure is not initially at rest. MODE-ID has been used successfully to identify modes of the 12-rib flexible antenna testbed produced by sine-sweep tests, as well as bridges and offshore platforms subjected to earthquakes.<sup>10-12</sup>

The MODE-ID program estimates the modal parameters by using a least-squares output-error method to minimize the error between the measured and the model output response to the recorded input excitation. MODE-ID uses a combination of a successive relaxation method and a modified steepest-descent method to minimize the error function with respect to the modal parameters. In practice, implementation of MODE-ID first requires the user to impose the number of predominant modes  $M$  to be identified in the measured response, and to select the initial estimates (usually from a numerical dynamic analysis) for the corresponding modal frequencies, damping, mode shapes, and participation factors. MODE-ID had no difficulty converging to the correct mode of the antenna when the sine-dwell test was tuned to the appropriate frequency and the measured signal was above the noise level.

#### IV. Numerical Model and Modal Sensitivity Analysis

##### Numerical Model

A finite element modal analysis of the testbed structure was performed with MSC/NASTRAN to investigate whether ML can be expected to occur in the structure and under what conditions. The model in Fig. 2 is comprised of 192 elements and 252 nodes, with six degrees of freedom per node. Each rib is divided into 10 identical beam elements. The studs are modeled as nine concentrated masses evenly spaced along each rib at the beam-element connection nodes. The pulley mechanism is represented by a simplified model using single-point and multiple-point constraints which is driven by the pulley counterweight and rotational inertia. Each inter-rib coupling wire is represented by two axial rod elements between the rib connection points, and each rod is elongated by a predetermined amount to generate the appropriate inter-rib tension. To form the geometric stiffness induced by the inter-rib coupling tension, five static-load iterations are performed. The modal analysis is then executed, and the first 36 modes are extracted.

The numerical model, although intentionally simple, is a close representation of the actual structure and includes the intrinsic small imperfections. To achieve this, the structural dimensions are measured directly off the existing structure when possible. Measured variations in the counterweight masses and inferred rib densities were found to be less than 5%, in accordance with ML requirements.

To avoid unnecessary complications in the numerical model, it was assumed that the ribs are rigidly connected to the hub, which is itself fixed against any type of motions. Potential modeling errors introduced by this assumption were investigated later. Because friction and stiction in the pulleys are almost impossible to model, the damping force is incorporated into the inertial forces of the pulley. The values of the pulley inertias used in the numerical model are obtained by matching the numerical modal frequencies of each rib to the results of the experimental single-rib tests. Differences in the frequencies

**Table 1 Band 1 and band 2 modal frequencies of the numerical 12-rib antenna model at nominal inter-rib coupling with no structural imperfections (all ribs have rib 1 properties), and with measured small imperfections obtained from the single-rib tests**

Mode no.	Modal frequency, Hz			
	Band 1		Band 2	
	Ideal	Imperfect	Ideal	Imperfect
1	0.220	0.216	1.516	1.473
2	0.228	0.224	1.519	1.479
3	0.228	0.225	1.519	1.491
4	0.249	0.246	1.526	1.493
5	0.249	0.247	1.526	1.499
6	0.275	0.270	1.536	1.503
7	0.275	0.273	1.536	1.506
8	0.299	0.294	1.545	1.509
9	0.299	0.296	1.545	1.518
10	0.315	0.309	1.552	1.525
11	0.315	0.313	1.552	1.534
12	0.321	0.320	1.555	1.555

are of the order of 1% for the first rib-bending mode, and 2% for the second rib-bending mode.

#### Numerical Modal Sensitivity Analysis

A modal analysis of the structure with nominal coupling tension and identical rib 1 properties was first performed. In this configuration, the structure does not have imperfections and is cyclically symmetric. The ensuing modal frequencies and mode shapes of the first 24 modes were computed (Table 1). For the ideal model,  $\Delta\lambda_1$  [Eq. (1)] equals 1.13, and  $\Delta\lambda_2$  equals 0.052. This implies that in its nominal coupling-tension configuration, the testbed will be much more sensitive to structural imperfections in the second band than in the first band, and will be theoretically more likely to display localization in band 2.

The modal deformations obtained from the model with the measured imperfections and coupled at the nominal inter-rib tension are illustrated in Fig. 3c for the umbrella mode of band 1 (i.e., mode 1-band 1), and Fig. 4c for the umbrella mode of band 2 (i.e., mode 1-band 2). In these figures, the solid line represents the undeformed structure and the dashed line represents the modal deformations. The modal frequencies of the actual model are listed in Table 1 along with those of the ideal model. The small imperfections of the ribs perturbed the degeneracy of the modal frequencies, creating pairs of closely spaced modes.

According to the numerical analysis, the band 1 modes are not significantly affected by the imperfections, although the modes at the edge of the band (e.g., modes 1 and 12) do exhibit slight irregularities. However, noticeable differences between the ideal and perturbed structural configurations can be observed in the band 2 modes, as predicted by the modal bandwidth values. For mode 1-band 2, the modal deformations are confined to ribs 5–12 (Fig. 4c). The numerical analysis also predicts strong localization for mode 12-band 2, the last mode of band 2, where the deformations are mainly confined to rib 10. However, the intermediate modes in the band are not expected to localize and should only exhibit small irregularities.<sup>1</sup> These results confirm previous investigations.<sup>2–8</sup> Hence, localization of the modes at the edge of band 2 should be observable by modal testing of the actual structure.

The sensitivity of the modal deformations and frequencies of the imperfect structure to variations in the inter-rib coupling tension was analyzed numerically. In addition to the nominal inter-rib coupling tension just described, the following inter-rib coupling configurations were considered: no inter-rib wires, coupling of 1/10, 1/4, 1/2 of the nominal coupling, and 2, 3, 4, and 10 times the nominal coupling. A summary of the resulting modal frequencies for band 1 and band 2 are listed in Table 2 for selected modes. The corre-

sponding modal deformations for the quarter- and triple-coupling configurations at mode 1-band 1 and mode 1-band 2 are illustrated in Figs. 3 and 4.

For this structure, the numerical sensitivity analysis of the coupling tension shows that the resulting modal bands which have a bandwidth  $\Delta\lambda_j$  [Eq. (1)] greater than 0.5 are not sensitive to structural imperfections and do not localize (Table 2). The analysis also confirms that the modal bandwidth decreases and the structure's susceptibility to ML increases as the band number increases and as the coupling stiffness decreases. The frequencies of the modes remain practically identical when the rib coupling is less than 50% of the nominal amount. In these cases, the geometric stiffness due to the small coupling tension is relatively negligible compared to the structural stiffness of the ribs. Furthermore, within a band of the perturbed model, the modes become more closely spaced as the inter-rib tension is decreased. For testing purposes, this implies that extracting the modal properties of the antenna testbed will be more intricate as the inter-rib stiffness is loosened and the variations between the rib properties become very small.

Inspection of the mode shapes shows that, as expected, each rib responds independently when there are no coupling wires. This case constituted an upper bound for the localized behavior of the actual testbed. When the inter-rib coupling tension is equal to 10% of nominal, only the umbrella mode and the 180 deg out-of-phase mode at the outer edges of band 1 are found to localize. The intermediate modes, although irregular, are still relatively extended throughout the antenna. However, for this same coupling configuration, all modes of band 2 are strongly localized and the deformations are mostly restricted to a single rib. As the inter-rib coupling is increased, the resulting localization effects are decreased. None of the band 1 modes localize for coupling levels larger than 50% of the nominal value, although the modal deformations are still somewhat irregular (Fig. 3). When the coupling is increased to three times the nominal value, only the modes at the edge of band 2 are localizing (Fig. 4). When the coupling is increased even further to 10 times the nominal values, all modes of the first two bands are fully extended. In this last case, the two structures differ in that the modes of the ideal one are degenerate, whereas those for the one with the existing small imperfections are well separated (Table 2). Hence, increasing the intercomponent stiffness in a cyclic structure with small imperfections will uncouple the modal frequencies but will preserve the mode shapes of the ideal structure.

## V. Test Procedure

### Preliminary Single-Rib Tests

To demonstrate the existence of ML, it is important to first verify that the imperfections between each of the ribs are sufficiently small. To this end, all of the inter-rib coupling wires were removed and each rib individually tested. The single-rib tests are also used to monitor abnormal variations in the damping resulting from friction and stiction in the ball-bearing pulleys, and are useful to construct a more accurate finite element model of the structure.

The single-rib dynamic tests consisted of sine sweeps performed between 0.01 and 2.5 Hz, and were designed to excite each rib in the first two bending modes. Using the data reduction software MODE-ID, the modal frequencies, damping, mode shapes, and participation factors for the first two bending modes of each rib were identified with one input time history at the root of the rib and two output histories at the levitator locations. The single-rib tests identified an average frequency for the first bending mode of the ribs at  $0.235 \text{ Hz} \pm 2\%$ , with a modal damping ratio of the order of 5%. The average frequency for the second bending mode is  $1.505 \text{ Hz} \pm 1\%$ , with a modal damping ratio of the order of 1%. These frequency variations correspond to overall structural imperfections of less than 5%, which satisfies the criterion of small imperfections for the ML experiments.<sup>2</sup> It will be shown

**Table 2** Sensitivity analysis of selected modal frequencies (Hz) of the 12-rib flexible antenna model with existing structural imperfections ( $\leq 4\%$ ) as a function of the inter-rib coupling tension; the nominal coupling tension is 4.45 N (0.5 lbf) at the outer-wire connection location and 2.22 N (1.0 lbf) at the inner-wire connection location

Coupling tension	Band 1 mode no.				Band 2 mode no.			
	1	2	3	12	1	2	3	12
Zero	0.230	0.230	0.230	0.246	1.480	1.487	1.489	1.549
10%	0.230	0.231	0.233	0.252	1.480	1.487	1.490	1.550
25%	0.228	0.231	0.233	0.264	1.480	1.486	1.490	1.550
50%	0.224	0.229	0.231	0.284	1.478	1.483	1.492	1.552
Nominal	0.216	0.224	0.225	0.320	1.473	1.479	1.491	1.555
$\times 2$	0.196	0.213	0.214	0.377	1.458	1.469	1.476	1.563
$\times 3$	0.173	0.200	0.201	0.422	1.442	1.456	1.461	1.573
$\times 4$	0.147	0.185	0.186	0.459	1.425	1.441	1.446	1.583
$\times 10$	—	0.095	0.095	0.714	1.317	1.347	1.355	1.725

**Table 3** Estimates of mode 1-band 1 and mode 1-band 2 from the sine-dwell tests performed on the 12-rib flexible antenna as a function of forced excitation levels and inter-rib coupling stiffness; modal frequencies (Hz) and damping (%) are evaluated with MODE-ID

Mode and coupling level	Sine-dwell forced excitation level							
	0.25 N		0.50 N		0.75 N		1.00 N	
	Frequency	Damping	Frequency	Damping	Frequency	Damping	Frequency	Damping
Mode 1-band 1								
No wires	0.236	1.59	0.235	1.30	0.234	1.31	—	—
25%	0.230	8.63	0.225	2.33	0.223	1.64	—	—
Nominal	—	—	0.216	2.63	0.214	1.68	0.214	1.95
$\times 3$	—	—	0.159	1.58	0.159	1.98	0.161	2.93
Mode 1-band 2								
No wires	1.490	0.88	1.490	0.86	1.490	0.89	1.492	0.95
25%	1.480	1.00	1.477	0.80	1.474	0.71	1.480	1.05
Nominal	1.475	0.66	1.472	0.57	1.469	0.52	1.475	1.14
$\times 3$	1.444	1.28	1.434	0.73	1.434	0.79	1.439	1.00

that even for perturbations this small, significant modal distortions can be observed.

#### Full-Dish Sine-Sweep Test

The next step in the ML experiment was to perform preliminary sine-sweep modal tests on the full structure, with the wires tensioned to the nominal-coupling values. The purpose of these tests was to approximately estimate the frequencies of the targeted second modal band and to verify whether ML can be observed. The forced harmonic excitation sweeps the frequency range between 1.4 to 1.7 Hz, and all of the rib-root actuators produce a signal of equal amplitude and phase, at a force of 1 N. This pattern should predominantly excite the lowest mode in the band (e.g., mode 1-band 2) in which the ribs of the perfect antenna are expected to vibrate in phase. If the structure had no imperfections, the response in the umbrella mode should have been the same at all of the ribs. However, analysis of the testbed behavior revealed significant differences in the response of the quasi-identical ribs.<sup>1</sup> Further experiments will verify that this mode is indeed localized.

Higher modes were also identified in this series of tests. Their mode shapes are compatible with the predicted deformation patterns of the inner-band modes with only slight irregularities. Although these modes are not localized, their behavior still remains consistent with ML theory.

#### Full-Dish Sine-Dwell Tests

From the preceding sine-sweep tests, mode 1-band 2 (i.e., second-bending umbrella mode) is chosen as the appropriate candidate for further investigation and verification of the variations in the parameters that govern ML. In accordance with ML theory, these experiments will verify whether mode-shape anomalies decrease as the inter-rib coupling increases, and whether mode 1-band 1 (i.e., first-bending umbrella

mode) displays, if at all, a lesser amount of modal disorder than mode 1-band 2. The results of the actual testbed and the numerical finite element model are compared to confirm the conclusions.

The flexible structure was sine-dwell tested at the tuned mode 1-band 1 and mode 1-band 2 frequencies, with a 12-rib in-phase forcing function, for four different coupling levels: nominal tension, quarter tension, triple tension, and zero tension (i.e., no wires connecting the ribs). The primary purpose of the zero-coupling test was to evaluate the amount of coupling transmitted through the rigidly clamped central hub by comparison with the finite element analysis results.

Each of these inter-rib stiffness configurations was also tested for different amounts of harmonic excitation force. Typically, the in-phase harmonic excitations were attempted at maximum force levels of 0.25, 0.50, 0.75, and 1.0 N. The aim was to verify whether significant nonlinearities govern the dynamics of the flexible antenna testbed and observe if they influence ML. The most likely sources of nonlinearities are the excessive deformations in the ribs and coupling wires resulting from large forcing levels, the stiction and friction in the pulleys, and possibly air drag from the flapping of the flexible ribs.

Finally, some of these test cases were reiterated to verify the repeatability of the results. This second series of sine-dwell tests were performed several months after the original tests. During that time the coupling wires were removed and adjusted to the appropriate stiffness many times. Hence, similarities in the results from the two series of tests add more credibility to the conclusions.

## VI. Test Results

More than 30 sine-dwell tests, with a 12-rib in-phase forcing pattern, were conducted to excite either mode 1-band 1 or mode 1-band 2 at four levels of inter-rib coupling and four

levels of excitation force. The tuning frequencies for the sine-dwell tests were dependent on the inter-rib coupling levels. The identified modal parameters are listed in Table 3, as a function of the inter-rib wire coupling and the forced excitation level. Instances where no estimates are given correspond to cases for which the excitation force was either too low to excite the mode above the encoder precision level, or too high and produced banging of the counterweights on the pulley casings.

#### Mode Localization as a Function of the Coupling Stiffness

Test results obtained from different amounts of inter-rib stiffness, but identical forcing levels, are compared to confirm that variations in the deformed mode shapes comply with the ML theory. Overlaid plots of the rib deformations for mode 1-band 2, at the inner sensor location where the response is the largest, are presented in Fig. 5 for decreasing levels of coupling strength. These mode shapes were obtained from sine-dwell tests at a 0.50-N excitation force, for which the response is expected to be least affected by poor signal-to-noise and nonlinear effects.

The sine-dwell tests performed for mode 1-band 2 validate the numerical analysis (Fig. 5). Regardless of the excitation-force level, localization is extreme when none of the wires connect the ribs, and only a small residual coupling may be transmitted through the suspension frame and the central hub. The predicted bandwidth for this particular case is  $\Delta\lambda_2 = 0.09$  [Table 3, Eq. (1)]. In this situation, only ribs 6 and 9 are

participating in the modal response at a frequency of about 1.49 Hz with 0.9% damping; all other ribs are at rest. As coupling is increased to the quarter-coupling and nominal-coupling cases, more modal response is observed in ribs 7 and 8 and the frequency is slightly decreased to about 1.48 and 1.47 Hz, respectively, with damping of the order of 0.7%. However, in both these cases, localization is still relatively strong. The predicted bandwidths for the quarter-coupling and nominal-coupling cases are, respectively,  $\Delta\lambda_2 = 0.10$  and 0.11 [Eq. (1)]. When the coupling is increased to the maximum level of three times the nominal configuration, localization is only marginal, although the response in some of the ribs is very low. For the triple-coupling case, the frequency of mode 1-band 2 dropped from 1.49 to 1.43 Hz and has an equivalent modal damping ratio of 0.8%. The predicted bandwidth for this particular case is  $\Delta\lambda_2 = 0.19$  [Eq. (1)]. It is anticipated that the ribs would progressively attain the same level of modal response throughout the antenna had it been possible to increase the inter-rib coupling strength even further.

For mode 1-band 1, the measured deformation is only slightly irregular (Fig. 9a) compared to the measured localized deformations for mode 1-band 2 (Fig. 9b). Regardless of the amount of inter-rib coupling, the first-bending umbrella mode does not localize.<sup>1</sup> However, the modal identification of band 1 was somewhat impeded by closeness of the modes and the restricted spectral accuracy of the measured data. Furthermore, the test results for mode 1-band 1 may have also been governed by the relatively high damping (1.3 to 2.6% modal damping) produced in part by the friction in the pulley ball bearings and possibly air drag. Damping was not included in the numerical analysis of the structure. A future objective may be to devise a ML indicator that not only uses the normalized bandwidth as a measure, but also incorporates modal damping.

#### Mode Localization as a Function of the Excitation Force

Variations in the mode shapes for the nominally coupled structure as a function of the excitation force are illustrated in Fig. 6 for mode 1-band 2. The disorder in the observed mode shapes decreases as the level of the forced excitation is increased. In general, increases in the excitation level are accompanied by slightly lower modal frequencies (Table 3). This is an indication that small nonlinearities, induced by excessive excitation levels, tend to soften the structure and decrease the ML effects. Increases in the modal frequencies observed for forces of 1.0 N are somewhat fictitious, since they are partially due to occasional banging of the pulley counterweights against the casings.

It also appears that the equivalent damping estimate is dependent on the excitation force level. As already speculated,

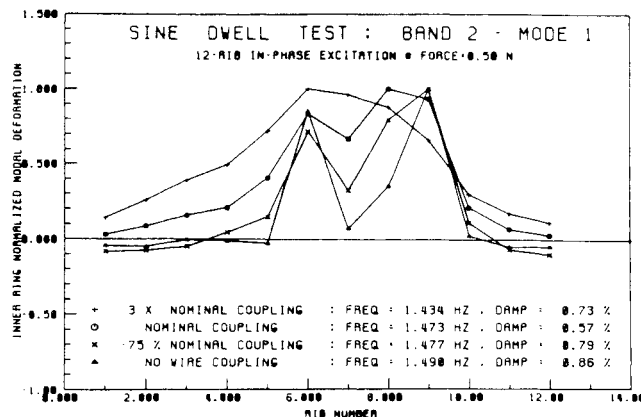


Fig. 5 Modal deformations of the imperfect 12-rib antenna for mode 1-band 2, obtained from sine-dwell tests with in-phase forced excitation at 0.5 N, as a function of inter-rib coupling tension for unwired, quarter, nominal, and triple coupling. The nominal tension is 4.45 N (1.0 lbf) at the inner ring and 2.22 N (0.5 lbf) at the outer ring.

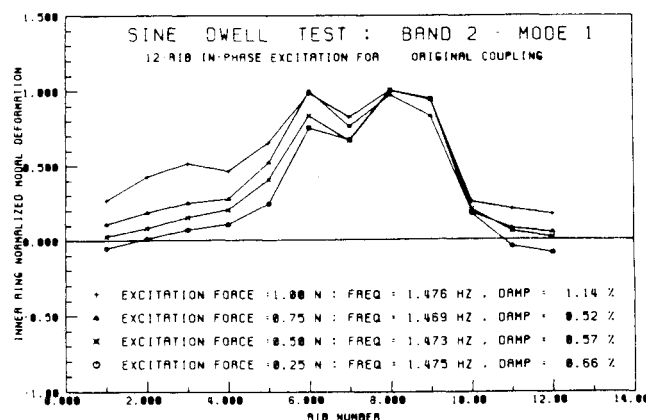


Fig. 6 Modal deformations of the imperfect 12-rib antenna with nominal inter-rib coupling for mode 1-band 2, obtained from sine-dwell tests with in-phase forced excitation at 0.25, 0.75, 0.50, and 1.0 N.

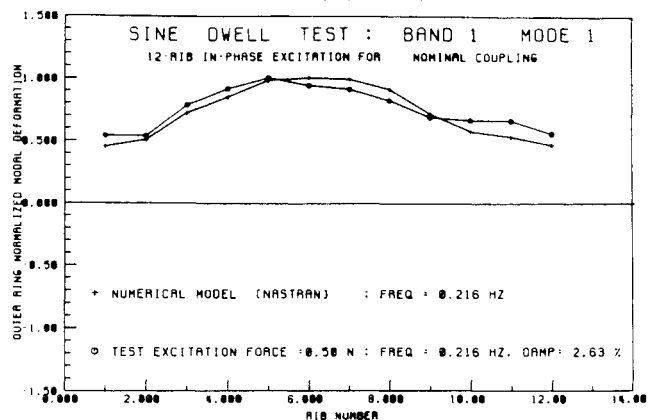


Fig. 7 Comparison between the numerical and experimental normalized deformation around the antenna with nominal coupling tension for mode 1-band 1 excited at 0.50 N.

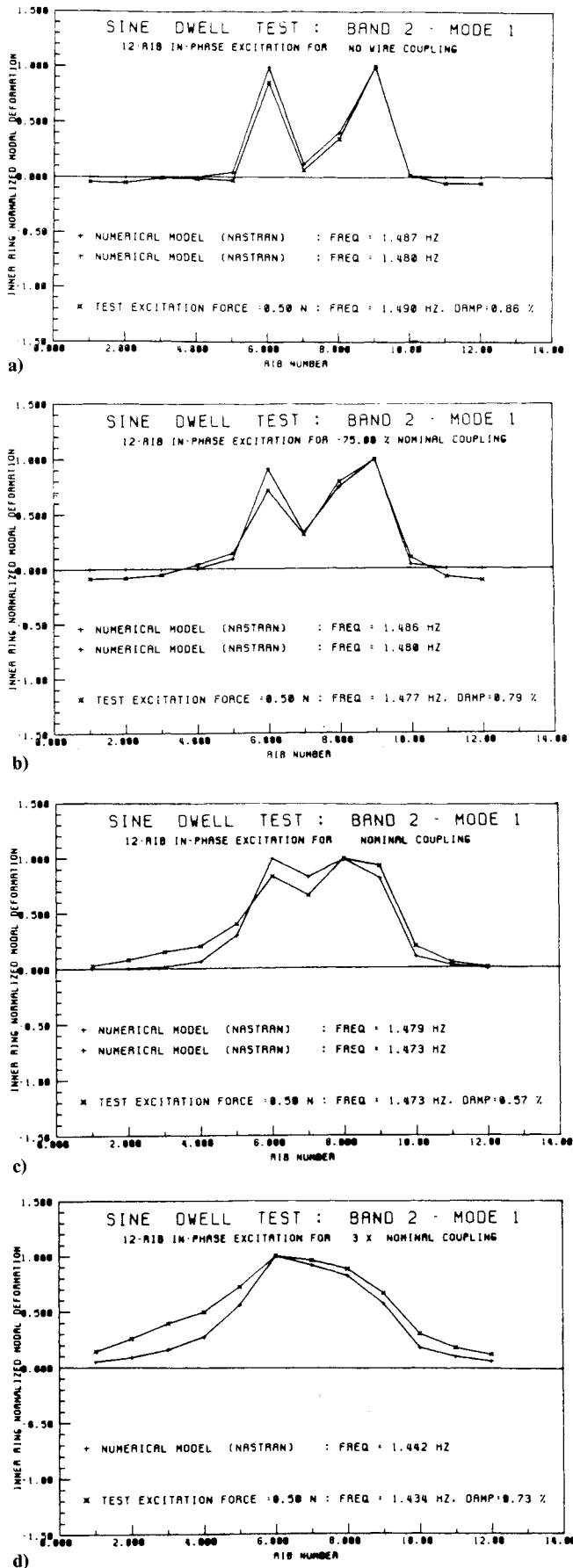


Fig. 8 Comparison of the experimental normalized deformation for mode 1-band 2 from in-phase sine-dwell tests at 0.5 N to the numerical model combining modes spaced within a 0.01-Hz interval, for coupling values of a) 10% nominal, b) 25% nominal, c) nominal, and d) 3x nominal.

high damping values may be a result of friction and stiction in the suspension pulleys, and of possible air drag of the vibrating ribs. However, these two sources of damping are independent of each other and usually do not affect the structure simultaneously by the same amount. Friction and stiction damping is generally expected to be more severe when the excitation forcing levels are low; damping estimates of the sine-sweep tests performed at the 0.25-N forcing level are larger than those for tests conducted at 0.50 or 0.75 N (Table 3). On the other hand, increased energy dissipation induced by the air drag for large motions leads to damping estimates for the 1.0-N tests which are larger than for the 0.5 or 0.75-N tests.

#### Comparison of Experimental and Numerical Results

The experimental and numerical results are compared to verify that the observations of ML in the actual structure conform with the analytical predictions. The experimental data obtained with a 0.5-N excitation force is used, since it is presumed to be the least affected by measurement noise and by nonlinear response of the structure and of the suspension mechanisms (Table 4). The numerical analysis did not include the effects of damping which could somewhat affect both ML and the modal response of closely spaced modes.

For the nominal inter-rib coupling case, the modal frequencies of the experimental structure and the numerical model for mode 1-band 1 and mode 1-band 2 match exactly at 0.216 and 1.473 Hz, respectively. Although the numerical model contained simplifying assumptions, the excellent fit of the full 12-rib model can be attributed in part to the identification of

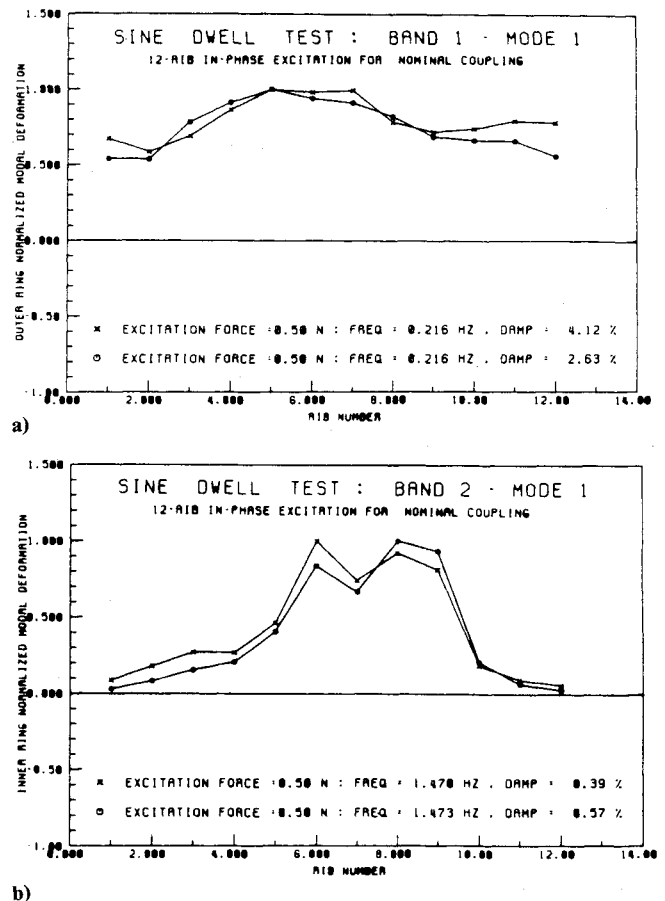


Fig. 9 Repeatability of the mode localization experiment: sine-dwell test of the 12-rib antenna with nominal coupling at 0.5-N excitation level for a) mode 1-band 1 and b) mode 1-band 2.



**Table 4 Modal frequencies (Hz) and damping (%) of the umbrella modes for the first two rib-bending modes; comparison between the numerical model and the identified results for the original and repeated sine-dwell tests at 0.50 N**

Ratio of nominal coupling	First umbrella mode rib first bending			Second umbrella mode rib second bending		
	F.E.M. model	Experiment	Repeat	F.E.M. model	Experiment	Repeat
No wires	0.230	0.235 (1.3%)	—	1.480	1.490 (0.9%)	—
25%	0.228	0.225 (2.7%)	0.228 (2.6%)	1.480	1.477 (0.8%)	1.475 (0.7%)
Nominal	0.216	0.216 (2.6%)	0.216 (4.1%)	1.473	1.472 (0.6%)	1.470 (0.4%)
× 3	0.173	0.159 (1.6%)	—	1.442	1.434 (0.8%)	—

the properties of the individual ribs and levitators in the finite element model which were experimentally measured and then numerically adjusted to match the results of the single-rib modal tests. The match in the modal frequencies for the other coupling cases are also excellent; the differences in the estimates are of the order of 2% for mode 1-band 1, and less than 0.5% for mode 1-band 2. The discrepancies are largest for the modes identified in the triple-coupling case, for which the simplifying assumptions in the numerical model may no longer be justified because of the much stiffer inter-rib coupling.

The numerical and experimental normalized mode shapes are compared for mode 1-band 1 at nominal coupling (Fig. 7), and for mode 1-band 2 at all levels of inter-rib coupling (Fig. 8). Minor discrepancies between the predicted and the measured mode shapes arose when the closely spaced modes were less than 0.01 Hz apart, which is also the spectral accuracy of the measured data. This situation occurs for loosely coupled configurations (Table 2). Using the principle of modal superposition, it was shown that for band 2 with coupling equal to the nominal values or less, MODE-ID identified the sum of the predicted first two closely spaced modes of the band (Figs. 8a–8c).<sup>1</sup> In the triple-coupling case, the frequency of mode 2-band 2 is more than 0.01 Hz above that of mode 1-band 2 (Table 3), and the spectral resolution is sufficient to separate the adjacent modes. As confirmed in Fig. 8d, only one mode is sufficient in the numerical model to obtain a good match with the experimental results. After making the corrections to account for the spectral accuracy of the measurements, the experimental and the predicted mode shapes matched very well (Fig. 8). It can be concluded that the testbed structure localizes and behaves as predicted numerically.

Slight differences remain in the amount of deformations observed in the quasistationary ribs, typically ribs 10–4, and the relative proportion of localized response shared by ribs 6 and 9. The extent of the discrepancy, although small, appears to be a function of the excitation force level used to conduct the sine-sweep test. These differences can be attributed to 1) the inability of the structure to reach full steady state in less than the maximum allowable testing time, 2) the approximate excitation forcing pattern which did not exactly duplicate the expected localized mode shape, and 3) damping in the actual structure which may be combining in the closely spaced modes in a slightly different way than predicted by the undamped numerical mode. In the triple-coupling case, the small differences may also be attributed to modeling approximations which may no longer be valid when the inter-rib tension approaches the buckling load. Nevertheless, the discrepancies in the observed deformations do not significantly affect the actual observations of ML in the structure.

A numerical sensitivity analysis concluded that the coupling transmitted through the stiffened central hub and the flexible suspension frame is equivalent to approximately 10% of the nominal inter-rib coupling.<sup>1</sup> This amount of coupling was shown numerically to be too small to make significant differences in the modal frequencies and deformations, was within

the bounds of experimental errors, and did not hinder the experimental observation of ML.

The results of the single-rib and the full-dish tests and analyses show that there is a definite correlation between the order in which the ribs localize within a band and the value of the modal frequencies of the individual ribs. According to the single-rib tests, the sequence of increasing frequencies for the second bending mode is rib 6, 9, 8, 7, 5, 3, 2, 11, 4, 1, 12, and 10, where ribs 6–9 are very closely spaced and are less than 0.015 Hz apart (Table 1). Hence, the antenna testbed is divided in two sectors, ribs 5–9 are the softest, whereas ribs 10–3 are the stiffest. This subdivision of the antenna testbed supports the experimental and numerical observations with regard to the lowest mode of the second bending group (i.e., mode 1-band 2), in which ribs 6–9 were most active dynamically, whereas ribs 10–4 were slower to react as the inter-rib coupling increased and the localization phenomenon decreased (Figs. 4 and 8). Furthermore, both the full-dish experimental and numerical results show that the sequence of localized deformations for increasing mode number is the same as that of the modal succession of the individual ribs just listed. This is most pronounced in the second modal band when the antenna is loosely coupled. Rib 6 dominates the deformations of the umbrella mode, and ribs 8 and 9 are the most active in mode 2 and mode 3. In the two highest modes of band 2, ribs 12 and 10 vibrate the most. Hence, good agreement of the experimental and analytical results prove that the modal frequencies of the individual quasi-identical elements can be used to predict the order of the localized modal formations within a band. This observation could be useful in future studies regarding delocalization or forced localization in specific sectors of a structure.

#### Repeatability of Results

The repeated sine-dwell tests were performed on the nominal- and quarter-coupling configurations at mode 1-band 1 and mode 1-band 2 for varying excitation force levels. For comparison, the identified modal frequencies and damping corresponding to these repeated tests are listed in Table 4, along with the modal results of the original set. For mode 1-band 1, the identified modal frequencies of the repeated tests are the same as the original experiments to within 0.003 Hz, which is far below the numerical accuracy of the data and represents a difference of only 1%. Damping for that mode is still large in both coupling cases. For mode 1-band 2, MODE-ID identified almost identical modal frequencies and damping for each repeated test in both the quarter- and nominal-coupling cases. The identified mode shapes also agree well, as compared in Fig. 9 for mode 1-band 1 and mode 1-band 2 at nominal coupling, where the overlaid modal deformations around the antenna are the results of the original and the repeated tests at 0.50 N. Consequently, the repeatability tests proved that the test procedures and the modal identification techniques used for the ML experiment provided consistent and reliable results.



## VII. Summary and Conclusions

The ML experiments successfully demonstrated that the phenomenon exists. The experimental results confirm that ML can be induced, observed, identified, and quantified in realistic space-like structures. The repeated tests produced similar results, and both numerical and experimental results agreed remarkably well. The most important conclusions of this study are summarized below.

1) A simple numerical model of the 12-rib testbed proved to be sufficient to predict the localized behavior of the structure.

2) The single-rib dynamic tests were extremely useful in determining the individual rib properties, the degree of rib imperfection, and the amount of damping induced by the complex levitation system. It was verified that the property imperfections within the structure were less than the 5% allowance required for the small-perturbation assumption. Furthermore, it was demonstrated that the order of the single-rib modal frequencies matched the sequence in which the ribs localized in the full structure.

3) Good agreement between the analytical and the experimental modal frequencies and deformations for the full structure confirmed that ML increases as a function of the decrease in the intercomponent coupling. For relatively low values of inter-rib coupling, localization effects in the second-bending umbrella mode became quite acute, restricting the dynamic response to a single rib. As the coupling was increased to higher levels, the antenna testbed still displayed irregularities in the modal deformations but was no longer localized.

4) Localization was more easily induced in the modes of the second bending group than in those of the first bending group. This agrees with the theoretical predictions which expect localization to become stronger with increasing modal bands, or equivalently, with decreasing modal bandwidth.

5) Although band 1 was numerically predicted to localize in the umbrella mode for loose coupling, high damping of the order of 2.5% induced by friction and stiction in the levitation system affected the combined response of the first four closely spaced modes and did not allow for immediate comparison with the undamped numerical results. The excessive damping could also be attenuating localization of the modes, as reported in past analytical investigations.<sup>8</sup> Nevertheless, damping in the second modal band, which is estimated to be slightly less than 1%, did not affect the match between the numerical and experimental modal estimates of that mode and did not impede the observation of the ML phenomenon.

6) Localization effects decrease as the forcing level of the harmonic excitation increases. Hence, nonlinearities in the testbed, such as stiction and friction of the suspension mechanism, large deformations of the ribs, and air drag induced by flapping, all contribute to reducing the expected disorder in the modal response. To date, all analytical investigations considered ML in linear structures. Future work should also be concerned with the localization of nonlinear structural systems.

Analytical studies have shown that localized modes can be expected to occur in a variety of large flexible space structures assembled from identical components. This not only encompasses the class of ribbed space reflectors used herein to perform the experiment, but also any kind of beam and truss construction which have loose translational or rotational coupling. Large space structures supporting precision instruments such as telescopes or interferometers are typically made of truss-type construction. Here, ML could affect the local modes of the vibrating struts and jeopardize the optical accuracy of the mirrors. Disregarding ML in these types of structures could lead to serious pointing and measurement errors, unstable vibrations and motions, as well as to possible cata-

strophic failure to excessive stress in concentrated areas of the structure. It is thus crucial to pursue research in this field and to investigate how mode localization affects control system designs, how it can be incorporated into the uncertainty modeling of the dynamic processes, or how it could be advantageously used to concentrate vibrational energy to selected sectors of a structure.

## Acknowledgments

The research described herein was performed by the Jet Propulsion Laboratory (JPL), California Institute of Technology, under contract with NASA. Funding was provided in part by A. Das, Air Force Phillips Laboratory, and by S. Venneri, NASA Office of Aeronautics and Space Technology, Code RM. The valuable help and discussions with A. Ahmed of JPL, P. Friedman and O. Bendiksen of the University of California at Los Angeles, and J. Beck of Caltech are gratefully acknowledged.

## References

- <sup>1</sup>Levine, M. B., and Salama, M. A., "Experimental Investigation of the Mode Localization Phenomenon," Jet Propulsion Lab., Internal Document D-8767, Pasadena, CA, Sept. 1991.
- <sup>2</sup>Bendiksen, O. O., "Mode Localization Phenomena in Large Space Structures," *AIAA Journal*, Vol. 25, No. 9, 1987, pp. 1241-1248.
- <sup>3</sup>Pierre, C., Tang, D. M., and Dowell, E. H., "Localized Vibrations of Disordered Multispan Beams: Theory and Experiment," *AIAA Journal*, Vol. 25, No. 9, 1987, pp. 1249-1257.
- <sup>4</sup>Cornwell, P. J., and Bendiksen, O. O., "Forced Vibration in Large Space Reflectors with Localized Modes," *Proceedings of AIAA/ASME/ASCE/AHS/ASC 30th Structures, Structural Dynamics, and Materials Conference* (Mobile, AL), AIAA, Washington, DC, 1989, pp. 188-198 (AIAA Paper 89-1180-CP).
- <sup>5</sup>Cornwell, P. J., and Bendiksen, O. O., "A Numerical Study of Vibration Localization in Disordered Cyclic Structures," *Proceedings of AIAA/ASME/ASCE/AHS/ASC 30th Structures, Structural Dynamics, and Materials Conference* (Mobile, AL), AIAA, Washington, DC, April 1989, pp. 199-208 (AIAA Paper 89-1181-CP).
- <sup>6</sup>Cha, P. D., and Pierre, C., "Vibration Localization by Disorder in Assemblies of Mono-Coupled, Multi-Mode Component Systems," *ASME Journal of Applied Mechanics*, Vol. 58, No. 4, 1991, pp. 1072-1081.
- <sup>7</sup>Lust, S. D., Friedman, P. P., and Bendiksen, O. O., "Mode Localization in Multi-Span Beams," *Proceedings of AIAA/ASME/ASCE/AHS/ASC 31st Structures, Structural Dynamics, and Materials Conference* (Long Beach, CA), AIAA, Washington, DC, April 1990, pp. 225-235 (AIAA Paper 90-1214-CP).
- <sup>8</sup>Lust, S. D., Friedman, P. P., and Bendiksen, O. O., "Free and Forced Response of Nearly Periodic Multi-Span Beams and Multi-Bay Trusses," *Proceedings of the AIAA/ASME/ASCE/AHS/ASC 32nd Structures, Structural Dynamics, and Materials Conference* (Baltimore, MD), AIAA, Washington, DC, April 1991, pp. 2831-2842 (AIAA Paper 91-0999-CP).
- <sup>9</sup>Vivian, H. C., Blaire, P. E., Eldred, D. B., Fleisher, G. E., Ih, C.-H. C., Nerheim, N. M., Scheid, R. E., and Wew, J. T., "Flexible Structure Control Laboratory Development and Technology Demonstration," Jet Propulsion Lab., Publication 88-29, Pasadena, CA, Oct. 1989.
- <sup>10</sup>Beck, J. L., "Determining Models of Structures from Earthquake Records," Earthquake Engineering Research Lab., Rept. EERL 78-01, Caltech, Pasadena, CA, June 1978.
- <sup>11</sup>Beck, J. L., "Statistical System Identification of Structures," *ASCE Proceedings International Conference on Structural Safety and Reliability* (San Francisco, CA), Aug. 1989.
- <sup>12</sup>Werner, S. D., Beck, J. L., and Levine, M. B., "Seismic Response Evaluation of Meloland Road Overpass using 1979 Imperial Valley Earthquake Records," *International Journal of Earthquake Engineering and Structural Dynamics*, Vol. 15, March 1987, pp. 249-274.
- <sup>13</sup>Levine-West, M., and Salama, M., "The Mode Localization Phenomenon: Visual Test Results," *International Video Journal of Engineering Research* (to be published).